

Human primordial germ cell commitment *in vitro* associates with a unique PRDM14 expression profile

Fumihiko Sugawa^{1,†}, Marcos J Araúzo-Bravo^{1,2,3,†}, Juyong Yoon^{1,†}, Kee-Pyo Kim¹, Shinya Aramaki¹, Guangming Wu¹, Martin Stehling¹, Olympia E Psathaki¹, Karin Hübner¹ & Hans R Schöler^{1,4,*}

Abstract

Primordial germ cells (PGCs) develop only into sperm and oocytes *in vivo*. The molecular mechanisms underlying human PGC specification are poorly understood due to inaccessibility of cell materials and lack of *in vitro* models for tracking the earliest stages of germ cell development. Here, we describe a defined and stepwise differentiation system for inducing pre-migratory PGC-like cells (PGCLCs) from human pluripotent stem cells (PSCs). In response to cytokines, PSCs differentiate first into a heterogeneous mesoderm-like cell population and then into PGCLCs, which exhibit minimal PRDM14 expression. PGC specification in humans is similar to the murine process, with the sequential activation of mesodermal and PGC genes, and the suppression of neural induction and of *de novo* DNA methylation, suggesting that human PGC formation is induced via epigenesis, the process of germ cell specification via inductive signals from surrounding somatic cells. This study demonstrates that PGC commitment in humans shares key features with that of the mouse, but also highlights key differences, including transcriptional regulation during the early stage of human PGC development (3–6 weeks). A more comprehensive understanding of human germ cell development may lead to methodology for successfully generating PSC-derived gametes for reproductive medicine.

Keywords BLIMP1; human pluripotent stem cells; primordial germ cell precursors; primordial germ cell specification

Subject Categories Development & Differentiation; Methods & Resources; Stem Cells

DOI 10.15252/embj.201488049 | Received 29 January 2014 | Revised 9 February 2015 | Accepted 18 February 2015 | Published online 6 March 2015

The EMBO Journal (2015) 34: 1009–1024

See also: **D Chen & AT Clark** (April 2015)

Introduction

There are two distinct germ cell specification modes in metazoans (Extavour & Akam, 2003; Johnson *et al*, 2003; Saitou & Yamaji, 2012). One is “epigenesis”, in which the germ cell lineage is specified from pluripotent embryonic cells (PSCs) by inductive signals from surrounding somatic cells. The other is “preformation”, in which the germ cell lineage is specified by the inheritance of localized determinants, the so-called germ plasm. Evolutionary studies have shown that the epigenesis mode is ancestral and widespread in metazoans (Extavour & Akam, 2003; Johnson *et al*, 2003; Saitou & Yamaji, 2012). In mice and probably in most other mammals, including humans, the germ line is determined by the epigenesis mode. In mice, classical embryological studies have shown that cells within the proximal epiblast begin their commitment to become alkaline phosphatase (AP)-positive primordial germ cells (PGCs) at the onset of gastrulation, between 5.5 and 6 days post-coitum (dpc) (Yoshimizu *et al*, 2001) in response to BMP signaling from the extraembryonic ectoderm (ExE) (Ginsburg *et al*, 1990; Lawson *et al*, 1999; Ohinata *et al*, 2009) and WNT signaling from the visceral endoderm (Ohinata *et al*, 2009). Investigations at the single cell level have revealed that PGCs share properties with their somatic mesodermal neighbors at onset of specification, as evidenced by the expression of the mesodermal factor *T* and *Hoxb1* (Saitou *et al*, 2002; Yabuta *et al*, 2006; Kurimoto *et al*, 2008). Subsequent repression of the somatic cell program and activation of the PGC program enable the emergence of PGCs with AP activity and expression of the PGC marker *Stella*. The mesodermal factor *T* downstream of WNT/BMP signaling was shown to be essential for specifying mouse PGCs and for directly regulating the germ cell determinants *Blimp1* and *Prdm14* (Aramaki *et al*, 2013). As *T* is activated in response to WNT3 before the activation of germ cell-specific genes, such as *Blimp1* (Liu *et al*, 1999; Rivera-Perez & Magnuson, 2005; Kurimoto *et al*, 2008), and is required for the specification of not only PGCs, but also other posterior mesoderm-derived tissues, such as the allantois and notochord (Gluecksohn-Schoenheimer, 1944; Yanagisawa *et al*, 1981; Wilson *et al*, 1995; Inman & Downs, 2006),

¹ Department of Cell and Developmental Biology, Max Planck Institute for Molecular Biomedicine, Münster, Germany

² Group of Computational Biology and Bioinformatics, Biodonostia Health Research Institute, San Sebastián, Spain

³ IKERBASQUE, Basque Foundation for Science, Bilbao, Spain

⁴ Medical Faculty, University of Münster, Münster, Germany

*Corresponding author. Tel: +49 251 70 365 300; Fax: +49 251 70 365 399; E-mail: office@mpi-muenster.mpg.de

[†]These authors contributed equally to this work

it is likely that some of the somatic cell program genes are required for proper PGC specification *in vivo*. This also suggests that PGCs are segregated from common mesodermal precursors by as yet unknown molecular mechanisms, with germ cells specified by epigenesis (Extavour & Akam, 2003). Molecular analysis has revealed that *Blimp1* and *Prdm14* are key factors in mouse PGC specification. They play an essential role in the repression of the somatic mesodermal program, activation of the PGC program, and global epigenetic reprogramming (Saitou et al, 2002; Yabuta et al, 2006; Seki et al, 2007). Furthermore, ectopic expression of *Blimp1* and *Prdm14*, together with *Tfap2c*, has been found to be sufficient for inducing mouse PGC-like cells (PGCLCs) from epiblast-like cells (EpiLCs) *in vitro*, supporting the notion that they play a dominant role in mouse PGC specification (Nakaki et al, 2013). Overexpression of *Prdm14* induces the formation of PGCLCs from only EpiLCs, but not from embryonic stem cells (ESCs), consistent with the role of *Prdm14* in safeguarding the maintenance of ESCs by preventing induction of extraembryonic endoderm fates and promoting expression of genes associated with ESC self-renewal (Ma et al, 2011). In addition, investigations on the molecular function of *Prdm14* have demonstrated that the factor interacts with the Polycomb Repressive Complex 2 (PRC2) to mediate the repression of diverse sets of genes via binding to H3K27me3, thereby ensuring a naïve ESC state. Knockout of *Prdm14* leads to the differentiation of ESCs toward a primed cell state in mice (Ma et al, 2011; Yamaji et al, 2013).

In humans, the molecular mechanisms underlying PGC specification at gastrulation (that is, 2–3 weeks of embryonic development) remain unclear, and a detailed analysis of gene expression dynamics during PGC specification has not yet been performed due to the lack of cell materials for experimental investigations. Nevertheless, immunochemical studies of carcinomas, germ cell tumors, and early-stage (10–15 week) germ cells have revealed that human germ cells and mouse PGCs exhibit similar expression profiles of a number of key genes, including *OCT4*, *NANOG*, *BLIMP1*, *TFAP2C*, *LIN28*, *SSEA1*, *CKIT*, *NANOS3*, *DAZL*, and *VASA*, like mouse PGCs (Castrillon et al, 2000; Gaskell et al, 2004; Anderson et al, 2007; Liu et al, 2007; Eckert et al, 2008; Kerr et al, 2008a,b; Julaton & Reijo Pera, 2011; Childs et al, 2012). These findings indicate the conservation of some germ cell signatures between both species. Furthermore, *CKIT*⁺ human PGCs have been shown to undergo whole-genome epigenetic reprogramming similar to mouse PGCs, indicating that common epigenetic modifications take place during PGC development in both species (Gkountela et al, 2013). However, the expression profiles and roles of key PGC genes, including *PRDM14* and *STELLA*, have not yet been fully defined in human germ cells. As in mouse, *PRDM14* appears to interact with PRC2 components in human ESCs and plays a crucial role in the maintenance of pluripotency (Chia et al, 2010). It binds to *OCT4* regulatory elements, thereby regulating *OCT4* expression and suppressing ESC differentiation. *PRDM14* is also thought to repress the expression of PGC-associated genes, such as *NANOS3* and *BMP4* (Chia et al, 2010). However, as mouse PGC specification is characterized by the re-acquisition of *Sox2* expression, the lack of *SOX2* expression in human PGCs suggests the notion that mechanistic differences exist between human and mouse germ cell formation (de Jong et al, 2008; Yamaji et al, 2008).

Over the past decade, several groups have reported on the generation of germ cell-like cells from human PSCs and the conservation

of specific genes and signaling cascades between humans and mice (Clark et al, 2004; Kee et al, 2006, 2009; Bucay et al, 2009; Park et al, 2009; Tilgner et al, 2010; Eguizabal et al, 2011; Medrano et al, 2011; Panula et al, 2011; Chuang et al, 2012). These studies demonstrate the importance as well as the potential of *in vitro* systems for investigating human germ cell development. Most studies have utilized the late-stage, post-migratory PGC marker *VASA/DDX4*, which is expressed in PGCs upon colonization of gonads but is not expressed in PGCs in earlier stages of development. This lack of a specific early germ cell reporter might explain why the characterization of human PGC specification and commitment *in vitro* has not been investigated until now. Mouse studies have shown that *in vitro*-derived *Blimp1*⁺ PGCLCs, which represent PGCs prior to 9.5 dpc, can generate functional sperm and oocytes after transplantation into mouse gonads (Hayashi et al, 2011, 2012). These early germ line committed cells have already acquired distinct, characteristic properties of PGCs. A defined *in vitro* system that enables the directed induction of pre-migratory PGCs is a prerequisite to understanding not only the mechanisms underlying early germ cell development, but also the methodology for successfully generating PSC-derived gametes.

Here, we describe a serum-free and defined differentiation procedure that can be used to generate pre-migratory PGCLCs from human ESCs and induced pluripotent stem cells (iPSCs). We have performed a comprehensive molecular analysis of PGCLCs and identified molecular events that take place during human germ cell commitment. Our results demonstrate that human germ cell specification *in vitro* shares key molecular mechanisms with the mouse system, but also that it exhibits unique mechanisms related to *PRDM14*.

Results

The combination of BMP4, Activin A, and bFGF promotes mesoderm-committed PGC-precursor formation from human PSCs

Serum-based PGC differentiation approaches are marked by undefined culture conditions and spontaneous cell differentiation, which are not suitable for investigating germ cell specification *in vitro*. In mice, PGC specification involves activation of the mesodermal program, as indicated by the expression of *T*, followed by activation of the PGC program, as indicated by the expression of germ cell determinant genes, such as *Blimp1* and *Prdm14* (Saitou et al, 2002; Kurimoto et al, 2008). The efficient generation of mesoderm-committed PGC precursors therefore supports the differentiation of lineage-restricted PGCs at a higher efficiency.

Treatment of human ESCs with a combination of Activin A (ActA) and BMP4 under serum-free conditions has been found to induce the formation of primitive streak-like cell populations and mesoderm (Yang et al, 2008). We thus sought to pre-differentiate human PSCs toward early mesoderm-committed PGC precursors with the help of these cytokines in the presence of bFGF for 2 days and to analyze the gene expression profiles of representative pluripotency-associated markers (*OCT4*, *NANOG*, and *SOX2*), PGC markers (*BLIMP1* and *STELLA*), and a mesodermal marker (*T*) (Fig 1A). *T* was rapidly upregulated by ActA and BMP4, whereas the expression of *OCT4*, *NANOG*, and *SOX2* did not change significantly. Based

on these profiles, we concluded that 20–50 ng/ml of ActA and 5 ng/ml of BMP4 were optimal for activating *T* expression (Fig 1A). Notably, *BLIMP1* (expressed from 6.5-dpc mouse PGCs) was concomitantly upregulated, whereas *STELLA* expression (expressed from 7.5-dpc mouse PGCs) was not significantly altered. This indicated the presence of a mesoderm-like cell state characterized by the expression of *T*. To determine whether differentiation for 2 days would be sufficient for maximizing the induction, we extended the differentiation period to day 7 and then analyzed the gene expression dynamics (Fig 1B). Over the entire culture period, expression levels of *OCT4*, *NANOG*, *SOX2*, and *STELLA* remained similar to those of iPSCs (we observed 0.5-, 0.5-, 2- and 2-fold changes, respectively). In contrast, *T* and *BLIMP1* were rapidly upregulated within the first 2 days (512- and 32-fold changes, respectively) and gradually downregulated thereafter. Interestingly, *T* was activated 1 day earlier than *BLIMP1*, suggesting the induction of a mesodermal progenitor-like state before germ cell activation, which is also observed in mice. *T* expression was detected on day 1 and *BLIMP1* expression on day 2, results that were confirmed by immunostaining (Fig 1C). At the protein level, *OCT4* was expressed in about 97% of all cells on day 0, and a small percentage (3%) of these PSCs expressed *T*. However, *BLIMP1* expression was not detected. Approximately 55% of *OCT4*⁺ cells expressed also *T* on day 1 (Fig 1D) and 58% on day 2, of which ca. 5% co-expressed *OCT4*, *BLIMP1*, and *T* (Fig 1D) and around 1% expressed only *OCT4* and *BLIMP1*. *STELLA*⁺ cells were not detected during precursor induction (Supplementary Fig S1A). These results are consistent with observations in mouse studies (Hayashi *et al*, 2011).

OCT4 and *BLIMP1* were still expressed at intermediate levels on day 7, suggesting that mesoderm-committed PGC precursors were still present at later time points of the differentiation (Fig 1B). However, immunofluorescence analysis revealed that *OCT4* and *BLIMP1* were no longer co-localized, indicating the loss of mesoderm-committed PGC precursors during prolonged culture *in vitro* (Supplementary Fig S1B). Overall, differentiation in defined medium conditions (N2B27 + ActA + BMP4 + bFGF + ROCK inhibitor (Y-27632)) for 2 days was sufficient for generating mesoderm-committed PGC precursors, that is, *OCT4*⁺/*Blimp1*⁺/*T*⁺ cells.

Of note, we did not detect cKIT protein in *OCT4*⁺ cells, although its transcript was significantly upregulated until day 7 (Supplementary Fig S1C), suggesting that the PGC precursors did not develop into lineage-restricted PGCs under the given culture conditions, but required a different environment to become PGCLCs.

PGC precursors differentiate toward PGCLCs with germ cell-specific marker expression

To obtain PGCLCs, we cultured d2 precursors in GMEM/20% KSR (GK20), containing BMP4, LIF, and Y-27632 (Fig 2A). A previous

study demonstrated that TRA-1-81⁺/cKIT⁺ populations represent post-migratory putative germ cells in humans (Gkoutela *et al*, 2013). We thus utilized that study's approach and isolated putative germ cell populations by monitoring TRA-1-81/cKIT expression. We first titrated for an optimal concentration of BMP4 required for the transition of the precursors toward PGCLCs. We observed that the number of TRA-1-81⁺/cKIT⁺ cells increased in a dose-dependent manner (from 7.3% to 24%) by day 4 (Fig 2B). A BMP4 concentration of 100 ng/ml (yielding 24% cells) was used thereafter to induce PGCLCs from precursors. Notably, in the absence of BMP4 (Fig 2B, no cytokine), approximately 7% of the cells were TRA-1-81⁺/cKIT⁺, representing a subpopulation of cells within the undifferentiated iPSC cultures that lacked germ cell gene expression, similar to observations in hESCs (Gkoutela *et al*, 2013).

The maximum number of TRA-1-81⁺/cKIT⁺ cells (20%) was observed on day 4 (Fig 2C). Thereafter, the number decreased steadily, with only 2.2% TRA-1-81⁺/cKIT⁺ cells detected on day 8. We attempted to increase the number of positive cells by adding stem cell factor (SCF) to the culture, but this proved to be insufficient (Supplementary Fig S2A). Nonetheless, about 5% precursors (Fig 1D) yielded on average 10–20% PGCLCs from hiPSCs and ca. 9% from hESCs, independent of the cell lines used (for example see Supplementary Fig S2B).

PGCLC characterization shows global progress of epigenetic reprogramming similar to *in vivo* PGCs

To validate the reliability and specificity of the TRA-1-81/cKIT marker combination for the isolation of PGCLCs in our system, we performed gene expression analysis for a subset of germ cell-specific markers in the cKIT⁺/TRA-1-81⁺ PGCLC population (Supplementary Fig S3A) and compared it to the cKIT⁺/SSEA1⁺ isolated cell population (Supplementary Fig S3B). The analyzed cell fractions exhibited similar gene expression, demonstrating their germ cell identity and vouching for the high fidelity of our isolation method (Fig 2D).

We then assessed the gene expression of *OCT4*, *NANOG*, *SOX2*, *BLIMP1*, and *STELLA* in the TRA-1-81⁺/cKIT⁺ PGCLCs. In contrast to cKIT⁻ populations, *BLIMP1* and *STELLA* were dramatically upregulated in PGCLCs, whereas *OCT4* and *NANOG* levels remained similar to iPSC levels. Upregulation of *BLIMP1* began on day 2 of differentiation, but *STELLA* was upregulated only after day 4 (Fig 3A), both at the RNA and protein levels (Fig 3B). Importantly, *SOX2* was downregulated in PGCLCs, which is typical of human PGCs (Fig 3A). These findings strongly suggest that PGCLCs represent *in vitro* counterparts of natural human PGCs.

During PGC development, epigenetic reprogramming occurs globally and in a locus-specific manner (Seki *et al*, 2007; Gkoutela *et al*, 2013; Kagiwada *et al*, 2013). Therefore, we assessed the erasure of DNA methylation at regulatory regions of imprinted *loci*

Figure 1. Induction of OCT4⁺/BLIMP1⁺ PGC precursors from human iPSCs.

- A Effects of ActA and BMP4 on the expression of selected pluripotency, PGC, and mesodermal genes during PGC-precursor induction. DM: dorsomorphin, SB: SB431542. Samples were calibrated with iPSC values, and iPSC values depict 1. Y-axes are in log₂ scale.
- B Gene expression dynamics of selected pluripotency, PGC, and mesodermal genes during prolonged PGC-precursor induction of up to day 7. Y-axes are in log₂ scale.
- C Immunofluorescence analysis for OCT4 (red), BLIMP1 (green), and T (white) on days 0, 1, and 2. Nuclei were stained with Hoechst (blue). The culture contained BMP4 (5 ng/ml), Activin A (50 ng/ml), and bFGF (20 ng/ml). Scale bar: 100 μm.
- D Quantification of respective cell populations shown in (C).
- Data information: Data are presented as means ± SD (*n* = 3).

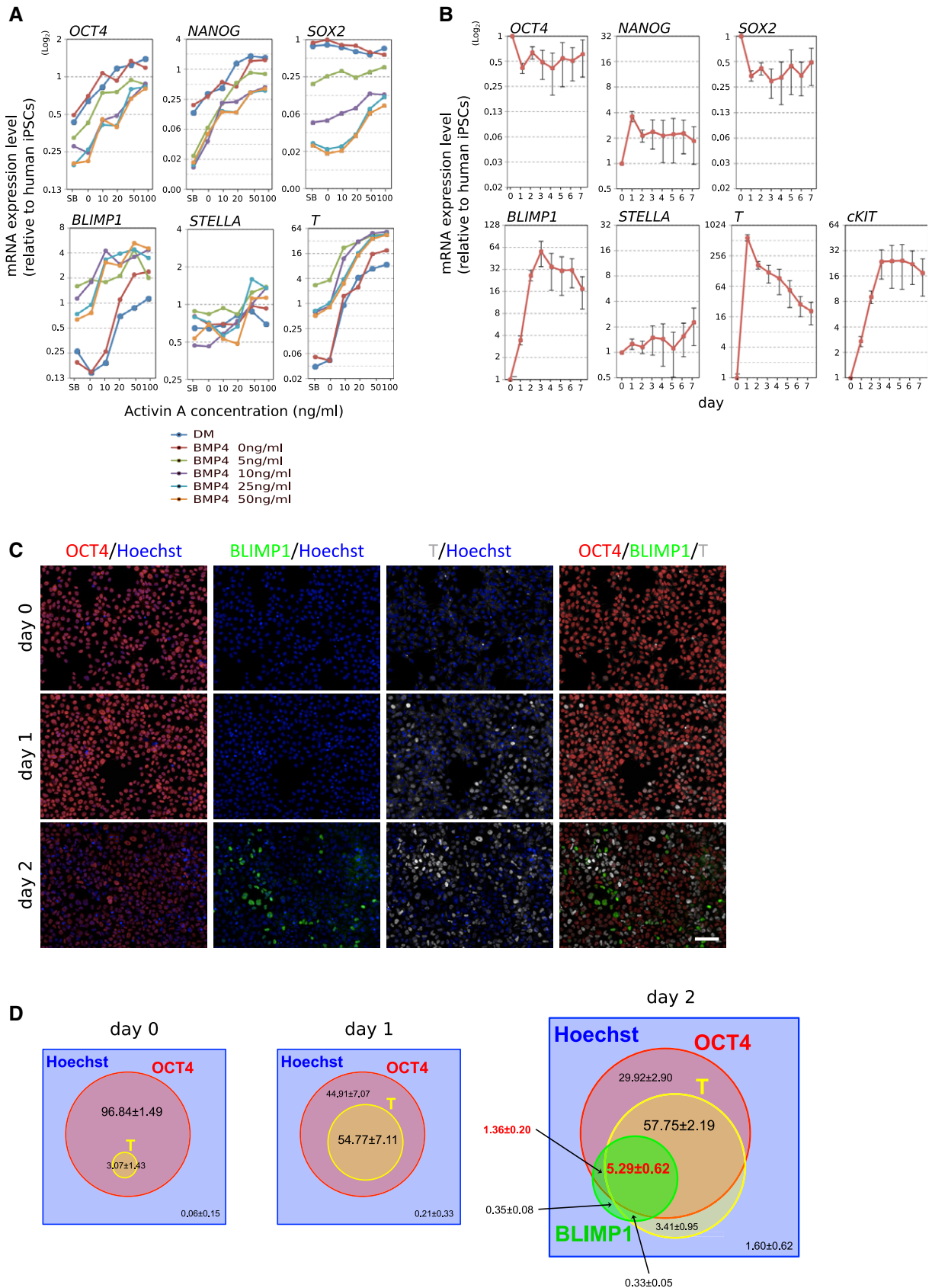


Figure 1.

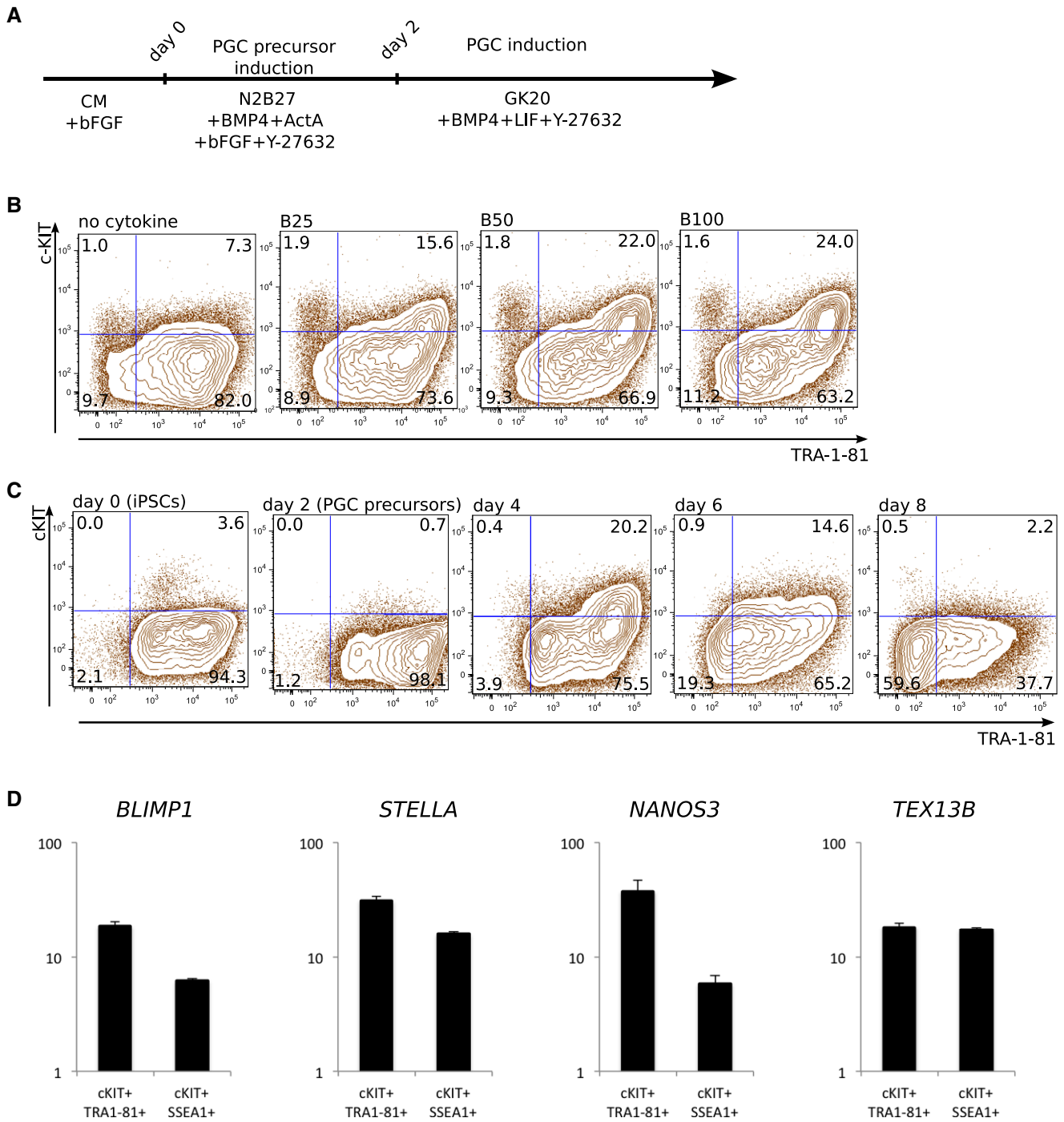


Figure 2. Induction of PGCLCs from human iPSCs.

A Schematic presentation of PGC-precursor and PGCLC induction.

B FACS analysis of the concentration-dependent effect of BMP4 on TRA-1-81⁺/cKIT⁺ PGCLCs on day 4. B25: 25 ng/ml BMP4; B50: 50 ng/ml BMP4; B100: 100 ng/ml BMP4.

C FACS analysis of TRA-1-81 and cKIT during PGC induction of up to day 8.

D Gene expression analysis of selected PGC markers in TRA-1-81⁺/cKIT⁺ and SSEA1⁺/cKIT⁺ FACS fractions of d4 PGCLCs. Samples were calibrated with iPSC values, and iPSC values depict 1.

Data information: Data are presented as means ± SD (n = 3).

and globally in PGCLCs. We found that *PEG1*, *KvDMR1*, *PEG10*, and *NESP55* were differentially methylated in both maternal and paternal alleles of iPSCs. With the exception of *KvDMR1*, both

alleles became demethylated in PGCLCs (Fig 3C). Furthermore, examination of global DNA methylation by immunofluorescence against 5-methyl-cytosine (5mC) showed that DNA was globally

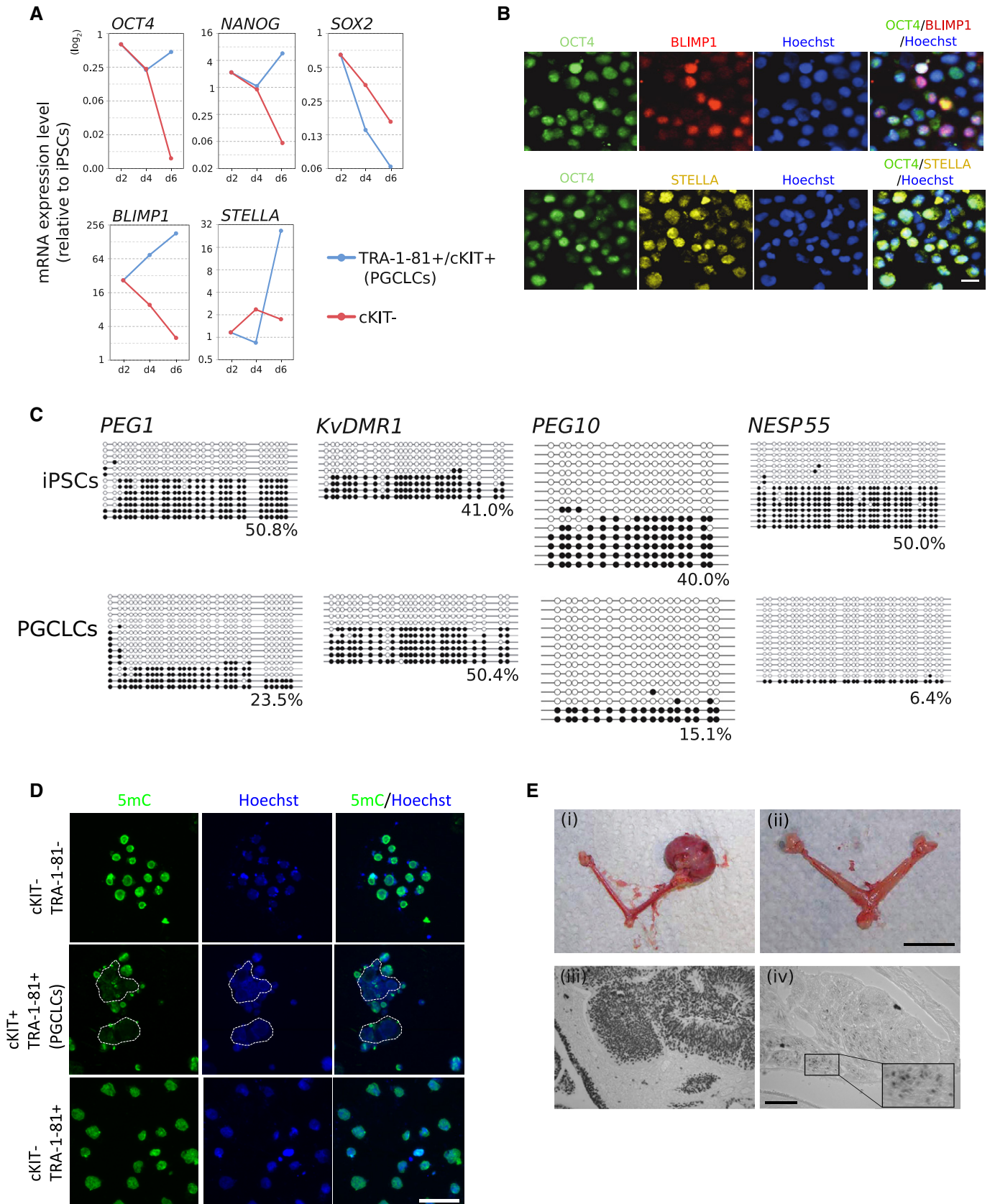


Figure 3.

Figure 3. Characterization of PGCLCs.

- A Gene expression dynamics of selected pluripotency and PGC genes in FACS-sorted, specified cells during PGC induction. The value for iPSCs is set as 1, and values are on \log_2 scale.
- B Immunofluorescence analysis for OCT4 (green), BLIMP1 (red), and STELLA (yellow) in TRA-1-81⁺/cKIT⁺ PGCLCs on day 6. Nuclei were stained with Hoechst (blue). Scale bar: 15 μ m.
- C Bisulfite sequence analysis of DMRs of the imprinted genes (*PEG1*, *KvDMR1*, *PEG10*, and *NESP55*) in iPSCs (top) and d6 TRA-1-81⁺/cKIT⁺ PGCLCs (bottom). White and black circles represent unmethylated and methylated CpG sequences, respectively.
- D Immunofluorescence analysis for 5mC in d6 PGCLCs. Nuclei were stained with Hoechst (blue). Scale bar: 50 μ m.
- E Transplantation of human iPSCs and PGCLCs into ovaries of recipient mice. (i) left ovary: control ovary without transplantation; right ovary: teratoma from iPSC-reconstituted ovary; (ii) PGCLC-reconstituted ovaries. Note that no teratomas had formed. Bottom panels: Immunohistochemical analysis for NUMA in sections of iPSC- and PGCLC-reconstituted ovaries. (iii) iPSC-induced teratoma shown in (i); (iv) ovary containing NUMA⁺ cells shown in (ii). Insert: higher magnification of selected area. Scale bars: (i) and (ii), 0.5 cm; (iii) and (iv), 50 μ m.

demethylated in PGCLCs (Fig 3D). Taken together, reduced methylated residues at imprinted loci and loss of methylcytosines in the genome both indicate the progress of epigenetic reprogramming in PGCLCs similar to PGCs *in vivo*.

We then evaluated the developmental potential of the PGCLCs. PGCs are bipotential, as they develop only into sperm and oocytes *in vivo*. To assess their potential, we attempted to transplant reconstituted ovaries. For this, PGCLCs or iPSCs, which were aggregated with 12.5-dpc mouse embryonic gonadal somatic cells to form reconstituted ovaries *in vitro*, were transplanted under the ovarian bursa of female mice. After 3 months, teratomas had formed from the reconstituted ovaries generated from iPSCs ($n = 2$) (Fig 3E[i and iii]), but not from the PGCLCs ($n = 10$) (Fig 3E[ii and iv]), indicating that PGCLCs are not pluripotent. To identify human cells within the ovarian grafts, we stained paraffin sections of the explants for human NUMA. As shown in Fig 3E[iv], NUMA-positive cells survived in the ovaries but apparently had neither proliferated nor differentiated much further. These cells were located close to the injection site and were distributed as single cells throughout this part of the tissue. We also did not observe mature PGCLCs, which might be attributed to a non-permissive environmental niche.

OCT4⁺/BLIMP1⁺ PGC precursors contribute to the subsequent generation of PGCLCs

WNT3, which is expressed in the mouse posterior visceral endoderm and epiblast, plays a crucial role in PGC specification (Ohinata *et al*, 2009; Aramaki *et al*, 2013), and the recombinant WNT signaling activator WNT3A enhances the differentiation of human ESCs into PGCs in the presence of serum (Chuang *et al*, 2012). In addition, knockout serum replacement (KSR) enhances the differentiation of cells into PGCLCs in mice by suppressing cell death during the transition of ESCs into epiblast-like cells (EpiLCs), which then further differentiate into PGCLCs (Hayashi *et al*, 2011).

Based on the above observations, we investigated whether KSR and WNT3A would also similarly influence PGC-like cell induction in our system. For this, we added KSR to the PGC-precursor medium at various concentrations (0–20%) and assessed the expression of *OCT4*, *SOX2*, *NANOG*, *T*, *BLIMP1*, and *STELLA* on day 2 (Fig 4A). *OCT4* and *NANOG* expression levels were similar in all tested samples, independently of the KSR concentration, whereas *SOX2* expression was strongly upregulated. *T* was similarly expressed at KSR concentrations between 0% and 4%, but its expression decreased dramatically in 10–20% KSR. *BLIMP1* expression gradually decreased in a concentration-dependent manner. We therefore

concluded that high concentrations of KSR inhibit the induction of PGC precursors by suppressing mesodermal gene activation. Importantly, *STELLA* expression was not affected by KSR, indicating that it did not enhance the induction of the PGCLC state. Protein expression of BLIMP1, OCT4, and T (Fig 4D), as determined by immunocytochemistry, matched the RNA expression results described above (Fig 4A). The majority of cells were OCT4⁺ under all conditions, whereas T⁺ cells were detected under only low KSR conditions (0–4%). BLIMP1⁺ cells were significantly induced under both low and high KSR conditions. However, BLIMP1⁺ cells did not co-express OCT4 under high KSR conditions (10–20%), indicating that they had apparently committed to a non-germ cell lineage (Fig 4D).

To assess the effect of WNT3A, we added 100 ng/ml of WNT3A to the PGC-precursor medium together with 0–20% KSR and determined the gene expression profiles. WNT3A did not drastically alter the expression of *OCT4*, *SOX2*, *NANOG*, *T*, *BLIMP1*, and *STELLA* (Fig 4A), or that of any tested ecto-/meso-/endoderm markers (Supplementary Fig S4), as all genes examined exhibited relatively similar levels and changes in their expression in either presence or absence of WNT3A. Thus, WNT3A did not enhance differentiation toward the mesodermal cell state in our system, but exhibited an antagonistic effect on the repression of mesodermal genes by KSR.

We then looked at the efficiency of PGCLC induction from each culture. The yield of TRA-1-81⁺/cKIT⁺ cells decreased with increasing KSR concentrations up to 4%, but increased again under high KSR conditions (10–20%) (Fig 4B). High KSR concentrations induced a cell population that did not express germ cell markers, except for cKIT, but expressed the hematopoietic markers *CD43* and *CD45*, indicating the cells' hematopoietic nature (Fig 4C). On the contrary, PGCLCs induced under standard conditions (0% KSR) expressed *BLIMP1* and *STELLA*, did not express hematopoietic marker genes, and showed a lower cKIT mRNA level than the hematopoietic cell fraction (Fig 4C). In addition, drastically reduced *Blimp1*/Blimp1 and *T*/T expression induced differentiation of cells into a non-germ cell fate (Fig 4A and D). Based on these data, we conclude that KSR and WNT3A do not enhance the induction of PGC precursors or PGCLCs in our system. KSR actually has an inhibitory effect and drives differentiation toward hematopoietic cells.

Transcriptomics analysis reveals that mesodermal and core PGC genes during human PGCLC induction and mouse PGC specification are similarly expressed

To further characterize d2 PGC-precursor cultures and d4 and d6 PGCLCs, we assessed their global gene expression profiles.

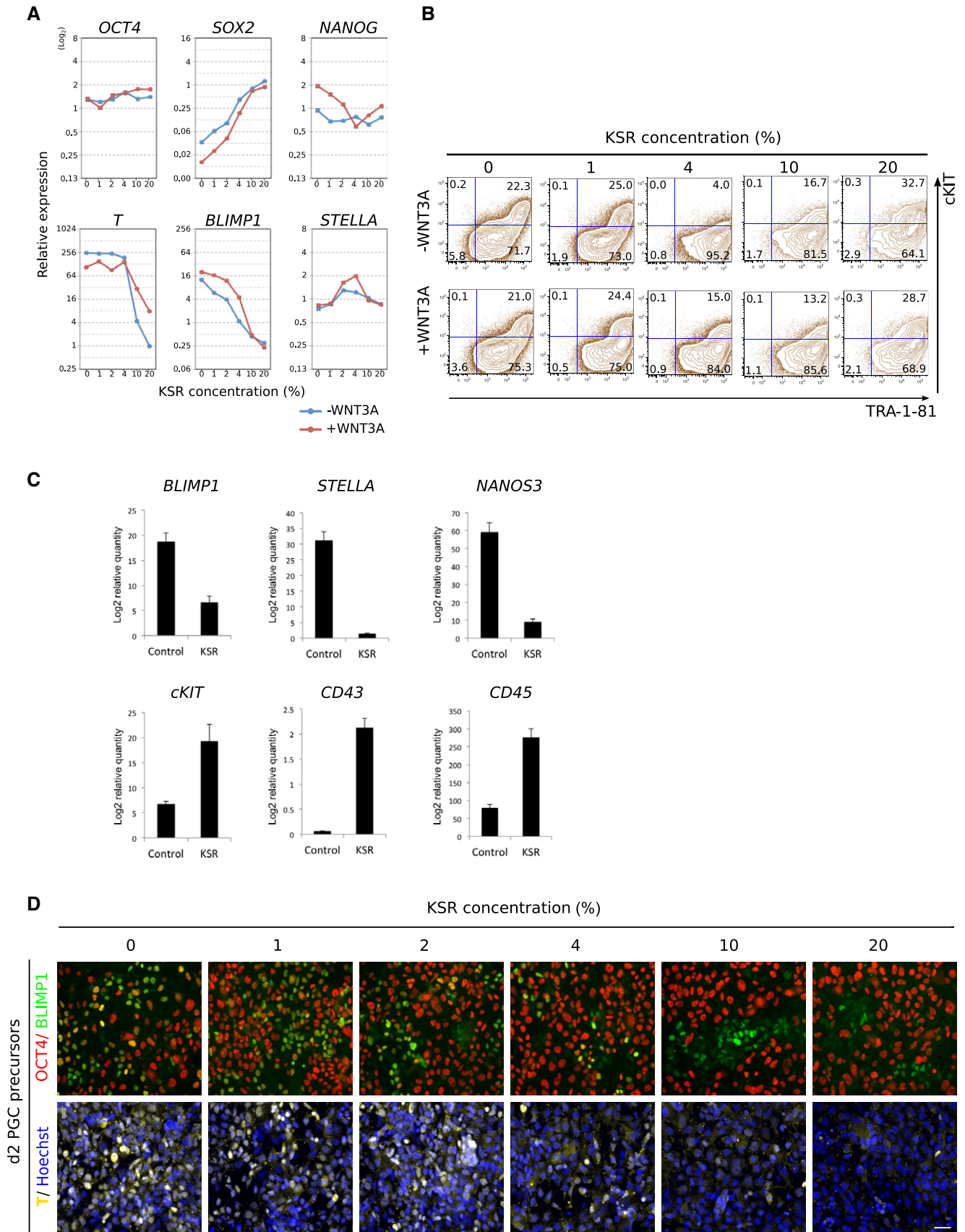


Figure 4.

Figure 4. Effects of KSR and WNT3A on PGC-precursor and PGCLC induction.

- A Effects of KSR and WNT3A during PGC-precursor induction on the expression of selected pluripotency, PGC, and a mesodermal gene of d2 cultures. The value for iPSCs is set as 1, and values are on log₂ scale. Data are presented as means ± SD (n = 3).
- B Effects of KSR and WNT3A on the induction of d6 PGCLCs as analyzed by FACS gated for TRA-1-81 and cKIT.
- C Gene expression analysis of selected PGC and hematopoietic markers in d6 PGCLCs that were cultured in 0% (control) or 20% KSR (KSR) condition during PGC-precursor induction. Samples were calibrated with iPSC values, and iPSC values depict 1. Data are presented as means ± SD (n = 3).
- D Immunofluorescence analysis for OCT4 (red), BLIMP1 (green), and T (yellow) in d2 precursors cultured in increasing KSR concentrations. Nuclei were stained with Hoechst (blue). Scale bar: 100 μm.

Unsupervised hierarchical clustering revealed that d2 PGC-precursor cultures clustered together with iPSCs and ESCs, whereas d4 and d6 PGCLCs clustered together but separately from d2 precursors and iPSCs (Fig 5A). Principal component analysis (PCA) also showed a clear difference of pluripotent stem cells (iPSCs and ESCs), d2 PGC-precursor cells, and d4 or d6 PGCLCs (Fig 5B). These results indicate that PGCLCs acquired a global gene expression profile that is distinct from that of pluripotent stem cells, demonstrating that the cell identities of both are different.

Scatter plots comparing either the d2 PGC-precursor culture, or d4 or d6 PGCLCs with iPSCs revealed that the global transcriptomics profile deviates progressively from that of the original iPSC population during differentiation, that *OCT4* and *NANOG* expression levels remained similar to those of iPSCs in all differentiated samples, and that *SOX2* was much lower in PGCLCs (Fig 5C). These results were confirmed by qPCR (Fig 1B). Mesodermal markers *CYP26A1*, *GSC*, *MESP*, and *MIXL1* were upregulated in d2 PGC precursors and thereafter progressively downregulated in d4 and d6 PGCLCs. PGC markers *STELLA*, *NANOS3*, and *TFAP2C* did not change in d2 PGC precursors and d4 PGCLCs, but significantly increased in d6 PGCLCs, indicating the formation of lineage-restricted PGCs on d6 (Fig 5C). The subsequent expression of mesodermal and PGC markers in our differentiation system was overall similar to the transcription dynamics observed during mouse PGC specification, with the exception of *SOX2*, which was drastically different.

We then analyzed the extent of shared expression dynamics between human PGCLC induction and mouse PGC specification. Nakaki *et al* (2013) identified two categories of genes that are activated during PGC specification in mice. One category is the “somatic mesodermal genes”, which are activated by BMP4 and eventually suppressed upon formation of lineage-restricted PGCs, and the other is the “core PGC genes”, which are specifically activated by *Blimp1*, *Prdm14*, and *Tfap2c*. We therefore examined the expression profiles of these genes from each category to assess whether similar transcriptional changes occur during human PGCLC induction (Supplementary Figs S5 and S6). Of 45 core PGC genes tested, 22 were upregulated (> 2-fold) in d6 PGCLCs, including *TFAP2C*, *STELLA*, *KLF2*, *ELF3*, *KIT*, and *LIFR*. This progression became nicely apparent in the violin plots (Supplementary Fig S5B). Of the 159 somatic mesodermal genes examined, 30 were upregulated (> 2-fold) in d2 precursor cells, including *CDX1*, *CDX2*, *HAND1*, *MESP1*, *ID1*, *MSX1*, *MSX2*, *ISL1*, *MIXL1*, *WNT5A*, *FGF8*, and *BMP4*. The number of upregulated genes increased to 50 on d4 and to 65 on d6, and this progression could also be demonstrated in violin plots (Supplementary Fig S6B). Thus, expression patterns of somatic mesodermal genes and core PGC genes during human PGC-like cell induction were similar to their expression patterns in mouse PGC specification. Taken together, human PGC-like cell induction and mouse PGC-like cell induction share expression patterns of not only a few

key markers, but also larger sets of genes within different functional categories.

In addition, *HOX* family genes, which are repressed by BLIMP1 in both mouse PGCs and human PGCLCs, showed low expression levels, and genes that regulate DNA methylation, *UHRF1*, *DNMT3A*, and *DNMT3B*, were downregulated in hPGCLCs (Fig 5E).

During the submission process of this manuscript, Irie *et al* (2015) reported that the endodermal factor *SOX17* functions in concert with *BLIMP1* as the key regulator of human PGCLC specification. Those authors reported that *SOX17* expression preceded *BLIMP1* expression and coincided with *T* expression (Irie *et al*, 2015). We analyzed d2 precursor cells and d4 and d6 PGCLCs and detected high *SOX17* expression in all samples (Supplementary Fig S7). These data support our findings and are in agreement with our conclusions on human germ cell specification *in vitro*.

Transcriptomics analysis suggests that mouse *Prdm14*-regulated genes are controlled by different mechanisms in human and mouse PGCs

We observed that *PRDM14* was strongly downregulated in human PGCLCs, but was highly expressed in mouse PGCLCs (Fig 5E). *Prdm14* functions as a key regulator of PGC specification and its depletion in mice leads to loss of PGCs (Yamaji *et al*, 2008). We therefore assessed whether the minimal *PRDM14* content in PGCLCs influences the expression of specific *Prdm14*-regulated genes (*Epas1*, *Tcl1*, *Esrrb*, *Klk5*, *Nr5a2*, *Zfp42*, *Klf4*, *Lifr*, *Dppa2*, *Dppa5a*, and *Nanog* upregulated; *Zfp521* [human homolog: *ZNF521*], *Sox3*, *Nrcam*, and *Hs6st2* downregulated) that are activated during mouse PGC specification (Nakaki *et al*, 2013). We first looked at their expression profiles in PGCLCs (Supplementary Fig S8). *EPAS1*, *KLF5*, *KLF4*, and *LIFR* expression levels were upregulated (> 2-fold), while *ZFP42* and *NANOG* levels did not change and remained as high as in iPSCs. However, *TCL1A*, *ESRRB*, *NR5A2*, *DPPA2*, and *DPPA5* levels were low. *ZNF521*, *SOX3*, and *NRCAM* levels were downregulated (> 2-fold) in PGCLCs, while *HS6ST2* was upregulated. These data clearly demonstrated that a subset of mouse *Prdm14*-regulated genes exhibits a similar expression pattern in human PGCLCs, even though *PRDM14* is expressed at only very low levels. In addition, gene ontology (GO) statistical enrichment analysis of differentially expressed genes (DEGs) between d6 PGCLCs and iPSCs revealed that neural development-related GO terms were significantly enriched by downregulated genes in PGCLCs (Supplementary Fig S9). The repression of neural differentiation is a key characteristic of mouse PGC specification that is mediated by *Prdm14*. These findings confirm that human PGCLC induction and mouse PGC specification exhibit similar transcriptional dynamics, and suggest that mouse *Prdm14*-regulated genes are differently regulated in human PGCs.

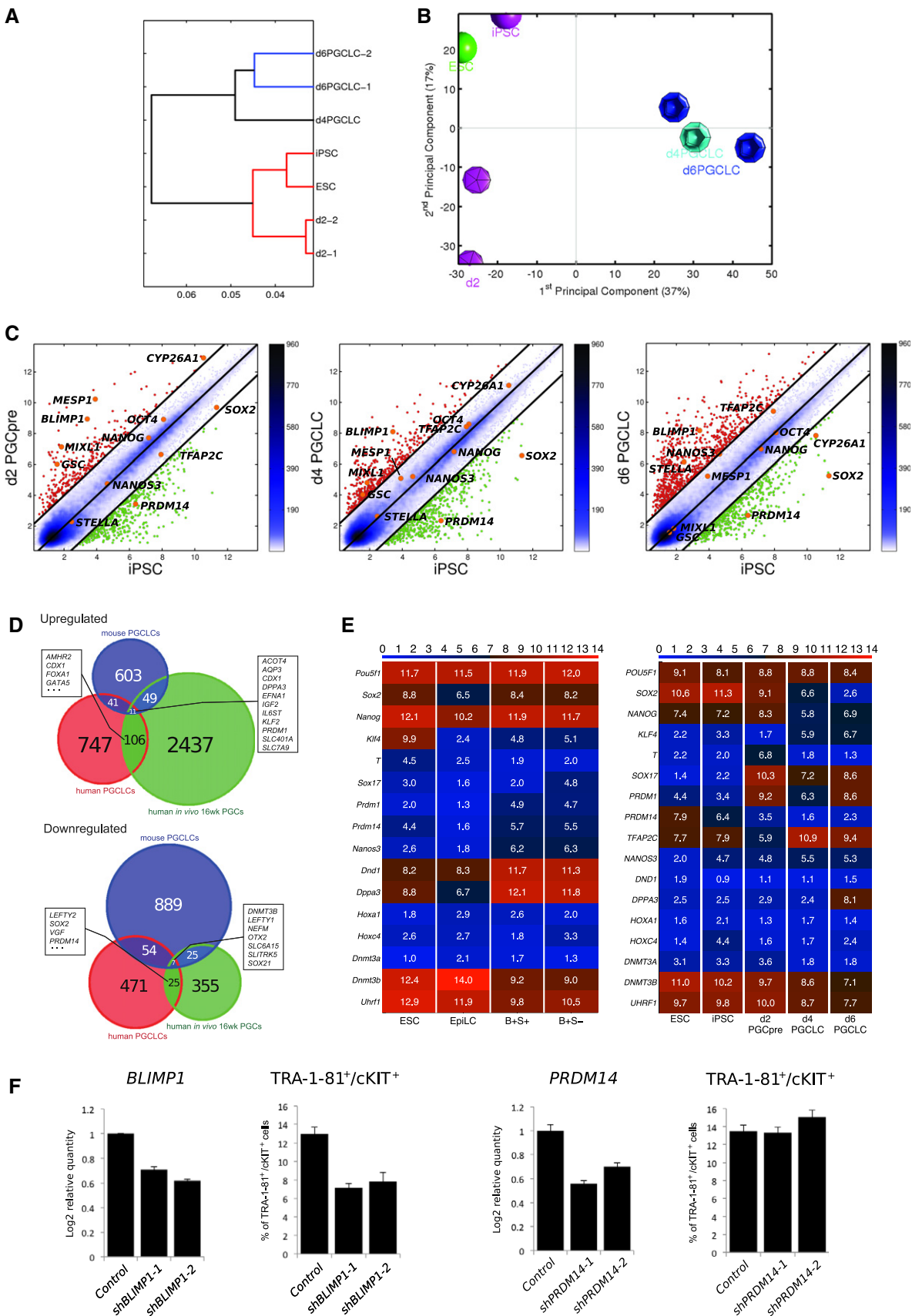


Figure 5.

Figure 5. Transcriptomics profiles during PGC-precursor and PGCLC induction.

- A Unsupervised hierarchical clustering of HuES6 ESCs, 383.2 iPSCs, d2 PGC-precursor cultures, and FACS-sorted PGCLCs.
- B Principal component analysis of HuES6 ESCs, 393.2 iPSCs, d2 PGC-precursor cultures, and FACS-sorted PGCLCs.
- C Scatter plots of global gene expression microarrays comparing d2 PGC-precursor cultures, or d4 or d6 FACS-sorted PGCLCs with iPSCs.
- D Venn diagrams of the transcriptomics meta-analysis with the intersections of the DEGs of mouse *in vitro* PGCLCs, human *in vivo* PGCs, and human *in vitro* PGC-like cells in relation to their respective pluripotent counterparts in their respective platforms.
- E Heatmap of pluripotent, germ cell, mesodermal, and chromatin-related markers in mouse (left) and human (right) transcriptomics samples (*Tfap2c* is not targeted in the Illumina MouseRef-8 v2). The color bars codify the gene expression in \log_2 scale. Red corresponds to high gene expression. *Blimp1*⁺*Stella*⁺ PGCLCs are denoted “B+S+”, and *Blimp1*⁺*Stella*⁻ PGCLCs are denoted “B+S-”.
- F Effect of knockdown of *BLIMP1* and *PRDM14* on PGCLC induction. Knockdown of *BLIMP1* (F) and *PRDM14* (G) was done using the lentiviral system with two individual shRNA vectors for each gene. The knockdown efficiencies were assessed by qPCR (left panel, each). The induction of d4 PGCLCs analyzed by FACS, gated for TRA-1-81 and cKIT (right panel, each). Data are presented as means \pm SD ($n = 3$).

To assess the influence of *PRDM14* and *BLIMP1* on PGCLC formation *in vitro*, we performed shRNA knockdown of *PRDM14* and *BLIMP1* in d2 precursor cells and analyzed TRA-1-81⁺/c-KIT⁺ PGCLCs formation on d4. *BLIMP1* knockdown to 60–70% reduced the percentage of PGCLCs by 50%, while *PRDM14* knockdown to 60–70% did not change the induction efficiency of PGCLCs at all, compared with the control sample (Fig 5F, Supplementary Fig S10). Comparison of *PRDM14/Prdm14* expression during the course of PGCLC differentiation from human and mouse PSCs demonstrated downregulation of *PRDM14* during precursor induction and no upregulation in human PGCLCs, while *Prdm14* levels decreased upon EpiLC induction in the mouse system and subsequently increased again in PGCLCs (Fig 5E). Immunocytochemical staining of *PRDM14* in precursor cultures on d1 and d2 confirmed the rapid loss of *PRDM14* at the protein level (Supplementary Fig S11).

***PRDM14* expression is very low from early commitment on to the post-migratory PGC stage in human**

With the unavailability of *in vivo* human pre-migratory PGC samples and transcriptomics data of those cells, we compared data from PGCLCs and iPSCs with published Next Generation Sequencing (NGS) data sets of *in vivo* human PGCs from Gkoutela et al (2013) and Nakaki et al (2013), and as a mouse counterpart, we used our own transcriptomics data of *in vitro* PGCLCs and EpiLCs. We performed a comparative gene expression meta-analysis and identified 7 and 11 genes that were commonly down- or upregulated, respectively, in PGCLCs, *in vivo* post-migratory PGCs, and mouse *in vitro*-generated PGCLC compared with the corresponding human ESC lines and EpiLCs (Fig 5E). Of these, *DNMT3B* was downregulated, indicating suppression of *de novo* DNA methylation, which is a common event at the early stage of PGC development in humans and mice. *BLIMP1*, *STELLA*, and *KLF2* were upregulated, while *SOX2* and *PRDM14* were downregulated in human PGCs and PGCLCs, but not in mouse *in vitro*-generated PGCs. These observations suggested that minimal *PRDM14* expression is a characteristic found in human but not in mouse PGCs from their early commitment to the germ cell lineage until at least the post-migratory stage.

Discussion

In this study, we describe a defined, serum-free two-step differentiation system using both human ESCs and iPSCs as starting cells. Our system allowed the reproducible induction of OCT4⁺/BLIMP1⁺/T⁺ PGC precursors that subsequently transitioned into

TRA-1-81⁺/cKIT⁺ pre-migratory PGCLCs. Such a stepwise induction for PGCLCs has been reported in a specification system for mouse (Hayashi et al, 2011). PGCLCs were induced from a heterogeneous cell population, which might be due to parameters or intrinsic differences that are not yet understood. This early-stage heterogeneity has also been observed in a mouse PGC induction study (Ohinata et al, 2009). This is very similar to how PGCLCs were induced in mouse differentiation systems, in which BMP4-induced PGCLCs comprised less than 50% of whole aggregates derived from EpiLCs (Hayashi et al, 2011) or less than 10% in serum-containing monolayer cultures, respectively (Hübner et al, 2003). The suggestion that PGCs are induced from common mesodermal progenitor cells confronts us with unknown regulatory mechanisms for the segregation of the germ cell lineage from the neighboring mesodermal somatic cells (Extavour & Akam, 2003; Aramaki et al, 2013).

Considering that spontaneous PGC differentiation from ESCs/iPSCs gives rise to only low numbers of PGCLCs, this two-step induction procedure generated a substantial number of pre-migratory PGCLCs for performing comprehensive molecular and biochemical analyses, constituting a new basis for further investigations.

Our data show that the combinatorial action of ActA, BMP4, and bFGF is critical for the first step of our system, that is, induction of OCT4⁺/BLIMP1⁺/T⁺ PGC precursors from human ESCs and iPSCs, which enables the subsequent robust induction of PGCLCs. Other studies have suggested that human ESCs and mouse EpiSCs share many features, such as morphology and gene expression profiles (Brons et al, 2007; Tesar et al, 2007). In the mouse system, BMP4 treatment of EpiSCs *in vitro* induced *Blimp1*⁺ cells, but most of these cells did not progress to become *Stella*⁺ PGC-like cells (Hayashi & Surani, 2009; Hayashi et al, 2011), suggesting that EpiSCs have low competence for PGC specification. However, when EpiSCs were reverted to ESC-like cells and subsequently induced into a pre-gastrulating mouse EpiLC state, they gained the ability to differentiate into *Blimp1*⁺/*Stella*⁺ PGCLCs in response to BMP4 (Hayashi et al, 2011). Considering that hESCs/hiPSCs generate PGCLCs cells through OCT4⁺/BLIMP1⁺/T⁺ precursors in our system, human ESCs/iPSCs might be composed of different subpopulations or might be more similar to a more naïve mouse pre-gastrulating epiblast state with high PGC differentiation ability, than to mouse EpiSCs. As we have shown previously, mouse epiblast stem cells contain distinct subpopulations (Han et al, 2010).

BMP4 played a critical role in the induction of PGCLCs and enhanced induction in a concentration-dependent manner in our culture system, similar to serum-based differentiation culture systems (Kee et al, 2006). Apart from BMP proteins, SCF and EGF have also been reported to enhance PGC induction in mice (Ohinata

et al, 2009). In particular, SCF is considered to be necessary for PGC survival (Pesce et al, 1993). We observed that the TRA-1-81⁺/cKIT⁺ PGCLC population declined dramatically upon culture beyond 6 days and our attempt to extend the proliferation of PGCLCs by SCF failed. According to the GO statistical enrichment analysis, lipid, hormone, and steroid metabolic processes were upregulated in d6 PGCLCs (Supplementary Fig S9). Therefore, the addition of hormones to the culture might be a more promising approach to extend and rescue human PGCLCs *in vitro*.

PGCLCs exhibited expression of *OCT4*, *NANOG*, *BLIMP1*, and *STELLA*, which is characteristic to mouse pre-migratory PGCs. We also confirmed by the analysis of whole-genome profiles that natural post-migratory human PGCs express high levels of *BLIMP1* and *STELLA*, similar to our human PGCLCs and mouse PGCs, which suggests that some of the key regulators of PGCs are conserved between these two species (Fig 5E). In addition, this analysis revealed that during differentiation, mesodermal genes, such as *T*, were initially upregulated in d2 PGC precursors and subsequently downregulated (Fig 5E). Concomitantly, PGC genes such as *BLIMP1*, *TFAP2C*, and *STELLA* were upregulated. This order of gene expression dynamics in association with hPGC specification is quite similar to that of mouse, in which *Blimp1* and *Prdm14* are activated after mesodermal gene activation (Fig 5E) (Saitou et al, 2002; Kurimoto et al, 2008). During mouse PGCLC specification *in vitro*, these genes are also not directly activated by BMP4. Instead, they are secondarily activated by the mesodermal transcription factor *T*, which is also an inducer of other mesodermal genes (Aramaki et al, 2013).

PGCLCs expressed low levels of *SOX2*, a typical feature of human PGCs of fetuses (de Jong et al, 2008; Perrett et al, 2008). The concomitant minimal expression level of *PRDM14*/*PRDM14* in our cells suggested that different regulatory mechanisms underlie human and mouse PGC specification and development (Fig 5E). In fact, we observed that post-migratory human fetal PGCs also exhibit very low expression levels of *SOX2* and *PRDM14* RNA, whereas mouse PGCLCs show high expression levels. These data suggest that human PGCs, from their early commitment to the germ cell lineage through at least the post-migratory stage, do not require *PRDM14*, or alternatively, that *PRDM14* is so critical in human, that low levels are tolerated and a complete loss would be necessary to reveal the phenotype. PGCs from *Prdm14*-deficient mice have been reported to exhibit low expression of *Sox2* (Yamaji et al, 2008), suggesting a potential genetic interaction of *Prdm14* and *Sox2* (Grabole et al, 2013). *Prdm14* also appears to play a key role in the repression of neural induction and *de novo* methylation, in addition to the activation of the PGC program in the mouse (Nakaki et al, 2013). In this context, our data revealed that human PGCLCs show: (i) the downregulation of genes associated with neural differentiation; (ii) similar expression dynamics to mouse *Prdm14*-regulated genes (such as *KLF5*, *NR5A2*, *KLF4*, *LIFR*, and *NANOG*); (iii) the progression of global epigenetic reprogramming by demethylation of differentially methylated regions (DMRs) of selective imprinted genes and a global decrease in 5mC levels; and (iv) the expression of *OCT4*, *NANOG*, and other pluripotency-associated genes. However, the mechanism underlying the regulation of these genes currently remains obscure.

Our differentiation protocol facilitates the generation of sufficient amounts of PGCLCs to investigate genetic interactions and epigenetic alterations. Moreover, we provide the first insights into transcriptional regulation during the early stage of human PGC

development (3–6 weeks), which are not found in mice. This underlines the importance of using human differentiation systems to understand the biology of the human germ cell lineage as well as specific reproductive problems. Continued investigations will provide a more comprehensive understanding of human germ cell development and an opportunity for performing research for reproductive medicine, such as drug screening and disease modeling by utilizing patient-specific iPSCs from reproductively compromised patients. We would like to eventually use it as a system to test toxic substances that might be a cause for the reduced fertility of men. Moreover, a more comprehensive understanding of human germ cell development may lead to methodology for successfully generating PSC-derived gametes for reproductive medicine.

Material and Methods

Cell culture

ESC lines (H9 and HuES6) and iPSC lines (393.2 and SA8/25) (Zaehres et al, 2010) were maintained in MEF-conditioned medium containing 5 ng/ml bFGF (Peprotech) on matrigel-coated plates (Greber et al, 2011) and used at a passage number below 50. The medium was changed every day, and the cells were passaged every 4–6 days by collagenase IV (1 mg/ml) dissociation of the culture into cell clumps.

Germ cell differentiation from human ESCs/iPSCs

To induce differentiation, ESCs/iPSCs were dissociated into single cells by TrypLE (Life Technologies) and plated on a matrigel-coated well of 12-well plates (2.0×10^5 cells/well) in N2B27 medium supplemented with BMP4 (5 ng/ml) (R&D Systems), Activin A (50 ng/ml) (R&D Systems), and bFGF (20 ng/ml), and ROCK inhibitor Y-27632 (10 μ M) (Abcam Biochemicals). Dorsomorphin (Santa Cruz, sc-200689) and SB431542 (Cayman Chemical Company) were used as controls at 50 nM and 10 μ M, respectively. After 48 h, cells were dissociated by TrypLE and plated in a well of ultra-low-attachment U-bottom 96-well plate (Corning) in GK20 medium (9,000 cells/well) supplemented with BMP4 (100 ng/ml), rhLIF (20 ng/ml) (Millipore), and Y-27632 (20 μ M). GK20 medium was GMEM supplemented with 20% KSR, 0.1 mM nonessential amino acids, 1 mM pyruvate, 0.1 mM 2-mercaptoethanol, 100 U/ml penicillin, and 100 mg/ml streptomycin.

Germ cell differentiation from mouse ESCs

Mouse ESCs (BVSC) were propagated under 2i-medium conditions, and PGCLCs were generated according to Hayashi et al (2011). Briefly, EpiLCs were induced from BVSC-ESCs on fibronectin-coated cell culture plates in N2B27 medium containing Activin A (20 ng/ml), bFGF (12 ng/ml), and KSR (1%) for 48 h. PGCLCs were induced by plating 1×10^3 EpiLCs in serum-free GK15 medium, supplemented with LIF (10^3 U/ml), SCF (100 ng/ml), BMP8a (500 ng/ml), BMP4 (500 ng/ml), and EGF (50 ng/ml) under floating conditions in ultra-low cell attachment U-bottom 96-well plates. Day-6 cultures were TrypLE-digested and sorted for BV and SC on a flow cytometer.

Fluorescence-activated cell sorting analysis

Aggregates were dissociated with 0.25% trypsin/EDTA supplemented with 2% chicken serum (37°C, 30 min). Dissociated cells were incubated with anti-TRA-1-81 antibody conjugated with phycoerythrin (FAB2155P; R&D Systems) and anti-cKIT antibody (17-1179; eBioscience) conjugated with APC (17-1179; eBioscience). Mouse IgG conjugated with APC (17-4714-82) and mouse IgM conjugated with phycoerythrin (ICo15P; R&D Systems) were used for isotype controls. The cells were washed three times with PBS supplemented with 5% FCS and analyzed on a flow cytometer.

Immunocytochemistry

Cells were fixed with 4% paraformaldehyde for 15 min, permeabilized with 0.2–1% Triton X-100 for 10 min, and blocked with a solution comprising 2% BSA, 5% FCS, and 0.1% Tween-20 in PBS for 45 min. For 5mC staining, FACS-sorted cells were attached to Superfrost Ultra Plus slides (Thermo Scientific) using a Cytospin centrifuge and stained for 5mC after treatment with 4 N HCl for 30 min at room temperature according to the manufacturer's recommendations. Primary and secondary antibodies were applied overnight at 4°C and for 1 h at room temperature, respectively, in 0.5% BSA in PBS-T. Hoechst stain was applied in the second-to-last washing step at 1 mg/ml. Antibodies used in this study were as follows: OCT4 (1:100, sc-5279; Santa Cruz), BLIMP1 (1:100, 9115; Cell Signaling), T (1:100, sc-17745; Santa Cruz), STELLA (1:100, MAB4388; Millipore), 5-MeCyd (1:100, AMM 99021; Aviva), and PRDM14 (1:100, AP1214a; Abgent) with the appropriate secondary antibodies: goat anti-mouse Alexa Fluor 488 (1:500, A11001; Invitrogen), donkey anti-mouse Alexa Fluor 647 (1:500, A31571; Invitrogen), donkey anti-rabbit Alexa Fluor 488 (1:500, A21206; Invitrogen), donkey anti-rabbit Alexa Fluor 568 (1:500, A10042; Invitrogen), donkey anti-goat Alexa Fluor 568 (1:500, A11057; Invitrogen).

Image acquisition and statistical cell counting

Images were acquired using the Leica inverted fluorescence microscope DMI6000AFC or the Operetta high-content imaging system (PerkinElmer, Waltham, MA, USA). Statistical cell counting was performed using the Harmony Software (PerkinElmer).

Immunohistochemistry

Paraformaldehyde-fixed paraffin sections were deparaffinized and rehydrated. For antigen retrieval, the slides were boiled in 10 mM sodium citrate buffer. Sections were pre-incubated in PBS and then blocked in 5% BSA and 1% normal goat serum in PBS at room temperature for 30 min. The sections were incubated with anti-NUMA antibody (ab84680, Abcam) in 1% BSA and 1% normal goat serum in PBS overnight at 4°C, and then incubated with biotinylated secondary antibody in 1% BSA and 1% normal goat serum in PBS (ab6828, Abcam) for 1 h at room temperature. For diaminobenzidine (DAB) staining, immunohistochemistry was performed using HRP streptavidin (405201, e-Bioscience) and Metal Enhanced DAB substrate kit (34065, Thermo Scientific). The DAB-stained preparations were visualized using a general optical microscope (Nikon TE-200U, Tokyo, Japan).

qPCR and microarray analysis

Total RNA was extracted from human ESCs/iPSCs, d2 PGC-precursor cultures, and d4 and d6 FACS-sorted PGCLC/non-PGCLCs, and mouse PGCLCs and EpiSCs and purified using the RNeasy Micro Kit (QIAGEN, Hilden, Germany). For qPCR, total RNA was reverse-transcribed by M-MLV Reverse Transcriptase (Affymetrix), and the resultant cDNA was used for Q-PCR analysis with iTaq Universal SYBR Green Supermix (Bio-Rad). The primer sequences used are listed in the Supplementary Table S1.

For transcriptomics microarrays, total RNA was used as input into a linear amplification protocol (Ambion), which involved synthesis of T7-linked double-stranded cDNA and 12 h of *in vitro* transcription incorporating biotin-labeled nucleotides. Purified and labeled cRNA was then hybridized for 18 h onto HumanHT-12 v4 expression BeadChips (Illumina) for human samples and on Mouse-Ref-8 v2 for mouse samples following the manufacturer's instructions. After washing as recommended, chips were stained with streptavidin-Cy3 (GE Healthcare) and scanned using the iScan reader (Illumina) and accompanying software. Samples were exclusively hybridized as biological replicates.

Microarray data processing

The bead intensities were mapped to gene information using BeadStudio 3.2 (Illumina). Background correction was performed using the Affymetrix Robust Multi-array Analysis (RMA) background correction model (Irizarry *et al*, 2003). Variance stabilization was performed using the \log_2 scaling, and gene expression normalization was calculated with the method implemented in the lumi package of R-Bioconductor. Data post-processing and graphics were performed with in-house developed functions in Matlab (MathWorks™). Hierarchical clustering of genes and samples was performed with one minus correlation metric and the unweighted average distance (UPGMA) (also known as group average) linkage method.

The GO terms were taken from the AMIGO gene ontology database (Ashburner *et al*, 2000). The significance of the GO terms of the DEGs was addressed calculating the *P*-values using an enrichment approach based on the hypergeometric distribution. All the sets of GO terms were back-propagated from the final term appearing in the gene annotation to the root term of each GO. The multi-test effect influence was corrected by controlling the false discovery rate using the Benjamini–Hochberg correction at a significance level $\alpha = 0.05$.

The data discussed in this publication have been deposited in NCBI's Gene Expression Omnibus and are accessible through GEO Series accession number GSE53498.

Transcriptomics meta-analysis

To build the human *in vitro* d6 PGCLC set, we performed transcriptomics analysis with Illumina HumanHT-12 v4 microarrays, taking the DEGs between d6 PGCLCs and the pluripotent iPSCs from which we derived the PGCLCs. To build the mouse *in vitro* PGCLC set, we performed transcriptomics analysis with Illumina MouseRef-8 v2 microarrays, taking the DEGs between mouse PGCLCs and the EpiLC reference pluripotent population. To build the human *in vivo* PGC set, we took the transcriptomics NGS data from Gkoutela *et al*

(2013) downloaded from the GEO database (GSE39821), and we used the cKIT⁺ 16-week PGC ovary sets (GSM979869, GSM979870) as representative human PGCs and the human H1 ESCs (GSM979871, GSM979872, GSM979872) as representative pluripotent cells to search for the DEGs. To calculate the DEGs, we used a threshold of 2 for the absolute values of the fold change in gene expression in log₂ scale for the Illumina microarrays transcriptomics data and a threshold of 4 for the higher dynamic range Illumina HiSeq 2000 NGS transcriptomics data. To build the Venn diagrams, the DEGs results were split between up- and downregulated DEGs.

Bisulfite sequencing

To determine the DNA methylation status at regulatory regions of imprinted genes, bisulfite conversion was carried out on 2 µg of isolated genomic DNA with the EpiTect Bisulfite Kit (QIAGEN) according to the manufacturer's protocol. The bisulfite-converted DNA was amplified by PCR using the primers previously described (Kim *et al*, 2007). The PCR products were cloned into the pCRII TOPO vector (Invitrogen) according to the manufacturer's protocol. Individual clones were sequenced by GATC-biotech (<http://www.gatc-biotech.com/en/index.html>). Sequences were analyzed using the Quantification Tool for Methylation Analysis (QUMA, <http://quma.cdb.riken.jp>).

Transplantation of reconstituted ovaries under the ovarian bursa

Generation of reconstituted ovaries and their transplantation under the ovarian bursa of mice was carried out according to a published protocol with slight modifications (Hayashi & Saitou, 2013). Briefly, FACS-sorted d4 TRA-1-81⁺/c-KIT⁺ cells were re-aggregated with embryonic day (E) 12.5 gonadal somatic cells at a ratio of 5,000:50,000. For this, the gonads of female embryos were collected at E12.5. The mesonephri were surgically separated from the gonads by using tungsten needles. The gonads were dissociated with 0.05% trypsin/0.02% DNase I (10–15 min, 37°C), and endogenous PGCs were removed by magnetic cell sorting using anti-SSEA1 antibody conjugated with magnetic beads (Miltenyi Biotec) according to the manufacturer's protocol. The resultant gonadal somatic cells and FACS-sorted PGCLCs were plated in the wells of a low-cell-binding U-bottom 96-well lipidure-coated plate in GK20. After 2 days of culture in GK20, the reconstituted ovaries were transplanted under the ovarian bursa. Briefly, two reconstituted ovaries were inserted with a glass capillary through a slit under the ovarian bursa of 4-week-old SCID female mice that had been anesthetized. Transplanted ovaries were then collected from the recipient female mice 3 months after transplantation.

Knockdown of *BLIMP1* and *PRDM14*

Knockdown experiments of *BLIMP1* and *PRDM14* were performed using the lentiviral system as described previously (Hockemeyer *et al*, 2008). TRC PRDM1 shRNA lentiviral vector (TRCN0000013608 and TRCN0000013609, Thermo Fisher Scientific) and TRC PRDM14 shRNA lentiviral vector (TRCN0000018523 and TRCN0000018525, Thermo Fisher Scientific) were used for the knockdown of *BLIMP1* and *PRDM14*, respectively. For infection of cells, d2 precursor cultures were pre-treated with 10 µM Y-27632 dihydrochloride for

1 h, and thereafter dissociated into single cells by TrypLE. 1×10^5 cells in 1 ml of precursor induction medium were infected with 60 µl of concentrated virus in 15-ml tubes and incubated at 37°C and 5% CO₂ for 5 h with occasional mixing. Thereafter, the cells were washed with PBS three times and used for further PGCLC induction. D4 PGCLC cultures were used for the assay.

Animal experiments

The xenotransplantation experiments were performed in accordance with the ethical guidelines and regulations of the German government (LANUV/Robert Koch Institut).

Supplementary information for this article is available online: <http://emboj.embopress.org>

Acknowledgements

We thank Martina Sinn and Bärbel Schäfer for assistance with the experiments, Boris Greber and Natalia Tapia for providing fruitful comments, Dirk Richter for figure preparation, as well as Areti Malapetsas for final editing. This work was supported by the Max Planck Society and the DFG grant for Research Unit Germ Cell Potential (FOR 1041).

Author contributions

FS, JY, KH, and HRS designed the experiments. FS, JY, MS, K-PK, GW, KH, and OEP performed the experiments. FS, JY, MJA-B, K-PK, and KH analyzed the data. FS, KH, MJA-B, K-PK, JY, SA, and HRS wrote the manuscript.

Conflict of interest

The authors declare that they have no conflict of interest.

References

- Anderson RA, Fulton N, Cowan G, Coutts S, Saunders PT (2007) Conserved and divergent patterns of expression of DAZL, VASA and OCT4 in the germ cells of the human fetal ovary and testis. *BMC Dev Biol* 7: 136
- Aramaki S, Hayashi K, Kurimoto K, Ohta H, Yabuta Y, Iwanari H, Mochizuki Y, Hamakubo T, Kato Y, Shirahige K, Saitou M (2013) A mesodermal factor, T, specifies mouse germ cell fate by directly activating germline determinants. *Dev Cell* 27: 516–529
- Ashburner M, Ball CA, Blake JA, Botstein D, Butler H, Cherry JM, Davis AP, Dolinski K, Dwight SS, Eppig JT, Harris MA, Hill DP, Issel-Tarver L, Kasarskis A, Lewis S, Matese JC, Richardson JC, Ringwald M, Rubin GM, Sherlock G (2000) Gene ontology: tool for the unification of biology. *Nat Genet* 25: 25–29
- Brons IG, Smithers LE, Trotter MW, Rugg-Gunn P, Sun B, Chuva de Sousa Lopes SM, Howlett SK, Clarkson A, Ahrlund-Richter L, Pedersen RA, Vallier L (2007) Derivation of pluripotent epiblast stem cells from mammalian embryos. *Nature* 448: 191–195
- Bucay N, Yebra M, Cirulli V, Afrikanova I, Kaido T, Hayek A, Montgomery AM (2009) A novel approach for the derivation of putative primordial germ cells and sertoli cells from human embryonic stem cells. *Stem Cells* 27: 68–77
- Castrillon DH, Quade BJ, Wang TY, Quigley C, Crum CP (2000) The human VASA gene is specifically expressed in the germ cell lineage. *Proc Natl Acad Sci USA* 97: 9585–9590
- Chia NY, Chan YS, Feng B, Lu X, Orlov YL, Moreau D, Kumar P, Yang L, Jiang J, Lau MS, Huss M, Soh BS, Kraus P, Li P, Lufkin T, Lim B, Clarke ND, Bard F,

- Ng HH (2010) A genome-wide RNAi screen reveals determinants of human embryonic stem cell identity. *Nature* 468: 316–320
- Childs AJ, Kinnell HL, He J, Anderson RA (2012) LIN28 is selectively expressed by primordial and pre-meiotic germ cells in the human fetal ovary. *Stem Cells Dev* 21: 2343–2349
- Chuang CY, Lin KI, Hsiao M, Stone L, Chen HF, Huang YH, Lin SP, Ho HN, Kuo HC (2012) Meiotic competent human germ cell-like cells derived from human embryonic stem cells induced by BMP4/WNT3A signaling and OCT4/EpCAM selection. *J Biol Chem* 287: 14389–14401
- Clark AT, Bodnar MS, Fox M, Rodriguez RT, Abeyta MJ, Firpo MT, Pera RA (2004) Spontaneous differentiation of germ cells from human embryonic stem cells *in vitro*. *Hum Mol Genet* 13: 727–739
- Eckert D, Biermann K, Nettersheim D, Gillis AJ, Steger K, Jack HM, Muller AM, Looijenga LH, Schorle H (2008) Expression of BLIMP1/PRMT5 and concurrent histone H2A/H4 arginine 3 dimethylation in fetal germ cells, CIS/IGCNU and germ cell tumors. *BMC Dev Biol* 8: 106
- Guizabal C, Montserrat N, Vassena R, Barragan M, Garreta E, Garcia-Quevedo L, Vidal F, Giorgetti A, Veiga A, Izpisua Belmonte JC (2011) Complete meiosis from human induced pluripotent stem cells. *Stem Cells* 29: 1186–1195
- Extavour CG, Akam M (2003) Mechanisms of germ cell specification across the metazoans: epigenesis and preformation. *Development* 130: 5869–5884
- Gaskell TL, Esnal A, Robinson LL, Anderson RA, Saunders PT (2004) Immunohistochemical profiling of germ cells within the human fetal testis: identification of three subpopulations. *Biol Reprod* 71: 2012–2021
- Ginsburg M, Snow MH, McLaren A (1990) Primordial germ cells in the mouse embryo during gastrulation. *Development* 110: 521–528
- Gkountela S, Li Z, Vincent J, Zhang K, Chen A, Pellegrini M, Clark A (2013) The ontogeny of cKIT+ human primordial germ cells proves to be a resource for human germ line reprogramming, imprint erasure and *in vitro* differentiation. *Nat Cell Biol* 15: 113–122
- Gluecksohn-Schoenheimer S (1944) The development of normal and homozygous brachy (T/T) mouse embryos in the extraembryonic coelom of the chick. *Proc Natl Acad Sci USA* 30: 134–140
- Grabole N, Tischler J, Hackett J, Kim S, Tang F, Leitch H, Magnúsdóttir E, Surani M (2013) Prdm14 promotes germline fate and naive pluripotency by repressing FGF signalling and DNA methylation. *EMBO Rep* 14: 629–637
- Greber B, Coulon P, Zhang M, Moritz S, Frank S, Muller-Molina AJ, Arauzo-Bravo MJ, Han DW, Pape HC, Scholer HR (2011) FGF signalling inhibits neural induction in human embryonic stem cells. *EMBO J* 30: 4874–4884
- Han DW, Tapia N, Joo JY, Greber B, Arauzo-Bravo MJ, Bernemann C, Ko K, Wu G, Stehling M, Do JT, Scholer HR (2010) Epiblast stem cell subpopulations represent mouse embryos of distinct pregastrulation stages. *Cell* 143: 617–627
- Hayashi K, Surani MA (2009) Self-renewing epiblast stem cells exhibit continual delineation of germ cells with epigenetic reprogramming *in vitro*. *Development* 136: 3549–3556
- Hayashi K, Ohta H, Kurimoto K, Aramaki S, Saitou M (2011) Reconstitution of the mouse germ cell specification pathway in culture by pluripotent stem cells. *Cell* 146: 519–532
- Hayashi K, Ogushi S, Kurimoto K, Shimamoto S, Ohta H, Saitou M (2012) Offspring from oocytes derived from *in vitro* primordial germ cell-like cells in mice. *Science* 338: 971–975
- Hayashi K, Saitou M (2013) Generation of eggs from mouse embryonic stem cells and induced pluripotent stem cells. *Nat Protoc* 8: 1513–1524
- Hübner K, Fuhrmann G, Christenson LK, Kehler J, Reinbold R, De La Fuente R, Wood J, Strauss JF 3rd, Boiani M, Schler HR (2003) Derivation of oocytes from mouse embryonic stem cells. *Science* 300: 1251–1256
- Hockemeyer D, Soldner F, Cook EG, Gao Q, Mitalipova M, Jaenisch R (2008) A drug-inducible system for direct reprogramming of human somatic cells to pluripotency. *Cell Stem Cell* 3: 346–353
- Inman KE, Downs KM (2006) Brachyury is required for elongation and vasculogenesis in the murine allantois. *Development* 133: 2947–2959
- Irie N, Weinberger L, Tang WW, Kobayashi T, Viukov S, Manor YS, Dietmann S, Hanna JH, Surani MA (2015) SOX17 is a critical specifier of human primordial germ cell fate. *Cell* 160: 253–268
- Irizarry RA, Hobbs B, Collin F, Beazer-Barclay YD, Antonellis KJ, Scherf U, Speed TP (2003) Exploration, normalization, and summaries of high density oligonucleotide array probe level data. *Biostat* 4: 249–264
- Johnson AD, Crother B, White ME, Patient R, Bachvarova RF, Drum M, Masi T (2003) Regulative germ cell specification in axolotl embryos: a primitive trait conserved in the mammalian lineage. *Philos Trans R Soc Lond B Biol Sci* 358: 1371–1379
- de Jong J, Stoop H, Gillis AJ, van Gurp RJ, van de Geijn GJ, Boer M, Hersmus R, Saunders PT, Anderson RA, Oosterhuis JW, Looijenga LH (2008) Differential expression of SOX17 and SOX2 in germ cells and stem cells has biological and clinical implications. *J Pathol* 215: 21–30
- Julaton VT, Reijo Pera RA (2011) NANOS3 function in human germ cell development. *Hum Mol Genet* 20: 2238–2250
- Kagiwada S, Kurimoto K, Hirota T, Yamaji M, Saitou M (2013) Replication-coupled passive DNA demethylation for the erasure of genome imprints in mice. *EMBO J* 32: 340–353
- Kee K, Gonsalves JM, Clark AT, Pera RA (2006) Bone morphogenetic proteins induce germ cell differentiation from human embryonic stem cells. *Stem Cells Dev* 15: 831–837
- Kerr CL, Hill CM, Blumenthal PD, Gearhart JD (2008a) Expression of pluripotent stem cell markers in the human fetal ovary. *Hum Reprod* 23: 589–599
- Kerr CL, Hill CM, Blumenthal PD, Gearhart JD (2008b) Expression of pluripotent stem cell markers in the human fetal testis. *Stem Cells* 26: 412–421
- Kee K, Angeles VT, Flores M, Nguyen HN, Reijo Pera RA (2009) Human DAZL, DAZ and BOULE genes modulate primordial germ-cell and haploid gamete formation. *Nature* 462: 222–225
- Kim K-P, Thurston A, Mummery C, Ward-van Oostwaard D, Priddle H, Allegrucci C, Denning C, Young L (2007) Gene-specific vulnerability to imprinting variability in human embryonic stem cell lines. *Genome Res* 17: 1731–1742
- Kurimoto K, Yabuta Y, Ohinata Y, Shigeta M, Yamanaka K, Saitou M (2008) Complex genome-wide transcription dynamics orchestrated by Blimp1 for the specification of the germ cell lineage in mice. *Genes Dev* 22: 1617–1635
- Lawson KA, Dunn NR, Roelen BA, Zeinstra LM, Davis AM, Wright CV, Korving JP, Hogan BL (1999) Bmp4 is required for the generation of primordial germ cells in the mouse embryo. *Genes Dev* 13: 424–436
- Liu P, Wakamiya M, Shea MJ, Albrecht U, Behringer RR, Bradley A (1999) Requirement for Wnt3 in vertebrate axis formation. *Nat Genet* 22: 361–365
- Liu Y, Wu C, Lyu Q, Yang D, Albertini DF, Keefe DL, Liu L (2007) Germline stem cells and neo-oogenesis in the adult human ovary. *Dev Biol* 306: 112–120
- Ma Z, Swigut T, Valouev A, Rada-Iglesias A, Wysocka J (2011) Sequence-specific regulator Prdm14 safeguards mouse ESCs from entering extraembryonic endoderm fates. *Nat Struct Mol Biol* 18: 120–127

- Medrano JV, Ramathal C, Nguyen HN, Simon C, Reijo-Pera RA (2011) Divergent RNA-binding proteins, DAZL and VASA, induce meiotic progression in human germ cells derived in vitro. *Stem Cells* 30: 441–451
- Nakaki F, Hayashi K, Ohta H, Kurimoto K, Yabuta Y, Saitou M (2013) Induction of mouse germ-cell fate by transcription factors in vitro. *Nature Cell* 137: 222–226
- Ohinata Y, Ohta H, Shigeta M, Yamanaka K, Wakayama T, Saitou M (2009) A signaling principle for the specification of the germ cell lineage in mice. *Cell* 137: 571–584
- Panula S, Medrano JV, Kee K, Bergstrom R, Nguyen HN, Byers B, Wilson KD, Wu JC, Simon C, Hovatta O, Reijo Pera RA (2011) Human germ cell differentiation from fetal- and adult-derived induced pluripotent stem cells. *Hum Mol Genet* 20: 752–762
- Park TS, Galic Z, Conway AE, Lindgren A, van Handel BJ, Magnusson M, Richter L, Teitell MA, Mikkola HK, Lowry WE, Plath K, Clark AT (2009) Derivation of primordial germ cells from human embryonic and induced pluripotent stem cells is significantly improved by coculture with human fetal gonadal cells. *Stem Cells* 27: 783–795
- Perrett RM, Turnpenny L, Eckert JJ, O'Shea M, Sonne SB, Cameron IT, Wilson DI, Rajpert-De Meyts E, Hanley NA (2008) The early human germ cell lineage does not express SOX2 during in vivo development or upon in vitro culture. *Biol Reprod* 78: 852–858
- Pesce M, Farrace MG, Piacentini M, Dolci S, De Felici M (1993) Stem cell factor and leukemia inhibitory factor promote primordial germ cell survival by suppressing programmed cell death (apoptosis). *Development* 118: 1089–1094
- Rivera-Perez JA, Magnuson T (2005) Primitive streak formation in mice is preceded by localized activation of Brachyury and Wnt3. *Dev Biol* 288: 363–371
- Saitou M, Barton SC, Surani MA (2002) A molecular programme for the specification of germ cell fate in mice. *Nature* 418: 293–300
- Saitou M, Yamaji M (2012) Primordial germ cells in mice. *Cold Spring Harb Perspect Biol* 4: pii: a008375
- Seki Y, Yamaji M, Yabuta Y, Sano M, Shigeta M, Matsui Y, Saga Y, Tachibana M, Shinkai Y, Saitou M (2007) Cellular dynamics associated with the genome-wide epigenetic reprogramming in migrating primordial germ cells in mice. *Development* 134: 2627–2638
- Tesar PJ, Chenoweth JG, Brook FA, Davies TJ, Evans EP, Mack DL, Gardner RL, McKay RD (2007) New cell lines from mouse epiblast share defining features with human embryonic stem cells. *Nature* 448: 196–199
- Tilgner K, Atkinson SP, Yung S, Golebiewska A, Stojkovic M, Moreno R, Lako M, Armstrong L (2010) Expression of GFP under the control of the RNA helicase VASA permits fluorescence-activated cell sorting isolation of human primordial germ cells. *Stem Cells* 28: 84–92
- Wilson V, Manson L, Skarnes WC, Beddington RS (1995) The T gene is necessary for normal mesodermal morphogenetic cell movements during gastrulation. *Development* 121: 877–886
- Yabuta Y, Kurimoto K, Ohinata Y, Seki Y, Saitou M (2006) Gene expression dynamics during germline specification in mice identified by quantitative single-cell gene expression profiling. *Biol Reprod* 75: 705–716
- Yamaji M, Seki Y, Kurimoto K, Yabuta Y, Yuasa M, Shigeta M, Yamanaka K, Ohinata Y, Saitou M (2008) Critical function of Prdm14 for the establishment of the germ cell lineage in mice. *Nat Genet* 40: 1016–1022
- Yamaji M, Ueda J, Hayashi K, Ohta H, Yabuta Y, Kurimoto K, Nakato R, Yamada Y, Shirahige K, Saitou M (2013) PRDM14 ensures naive pluripotency through dual regulation of signaling and epigenetic pathways in mouse embryonic stem cells. *Cell Stem Cell* 12: 368–382
- Yanagisawa KO, Fujimoto H, Urushihara H (1981) Effects of the brachyury (T) mutation on morphogenetic movement in the mouse embryo. *Dev Biol* 87: 242–248
- Yang L, Soonpaa MH, Adler ED, Roepke TK, Kattman SJ, Kennedy M, Henckaerts E, Bonham K, Abbott GW, Linden RM, Field LJ, Keller GM (2008) Human cardiovascular progenitor cells develop from a KDR+ embryonic-stem-cell-derived population. *Nature* 453: 524–528
- Yoshimizu T, Obinata M, Matsui Y (2001) Stage-specific tissue and cell interactions play key roles in mouse germ cell specification. *Development* 128: 481–490
- Zaehres H, Kogler G, Arauzo-Bravo MJ, Bleidissel M, Santourlidis S, Weinhold S, Greber B, Kim JB, Buchheiser A, Liedtke S, Eilken HM, Graffmann N, Zhao X, Meyer J, Reinhardt P, Burr B, Waclawczyk S, Ortmeier C, Uhrberg M, Scholer HR et al (2010) Induction of pluripotency in human cord blood unrestricted somatic stem cells. *Exp Hematol* 38: 809–818.e2



License: This is an open access article under the terms of the Creative Commons Attribution-NonCommercial-NoDerivs 4.0 License, which permits use and distribution in any medium, provided the original work is properly cited, the use is non-commercial and no modifications or adaptations are made.